

# Global Superdissolution of Weak Chaos

Itzhack Dana

Minerva Center and Department of Physics, Bar-Ilan University, Ramat-Gan 52900, Israel

## Abstract

A class of kicked rotors is introduced, exhibiting accelerator-mode islands and global superdissolution for arbitrarily weak chaos. The corresponding standard maps are shown to be exactly related to generalized web maps taken modulo an "oblique" cylinder. Generically, the global superdissolutive weak chaos arises as a perturbation of an analogous pseudochaotic behavior. In a particular case, it arises by folding stochastic webs back into the cylinder. The accelerator-mode islands are then essentially normal web islands folded back into the cylinder. This weak-chaos superdissolution thus appears to be basically different in nature from the strong-chaos one in standard and web maps.

PACS numbers: 05.45.Ac, 05.45.Mt, 45.05.+x

arXiv:nlin/0304048v1 [nlin.CD] 24 Apr 2003

The complexity and rich variety of dynamical behaviors of Hamiltonian systems with two degrees of freedom is well exhibited by simple 1D time-periodic models. A realistic paradigm is the kicked rotor with Hamiltonian  $H = \frac{p^2}{2} + V(x) \sum_{n=-1}^P \delta(t - n)$ , where  $p$  is angular momentum,  $x$  is angle on a circle  $S = [0; 2\pi)$ , and the potential  $V(x)$  is usually chosen as  $V(x) = \epsilon \cos x$ , being a nonintegrability parameter. The phase space is a cylinder and the values of  $(x; p)$  at integer times  $t = n = 0$  are related by the "standard" map [1,2]

$$S : p_{n+1} = p_n + f(x_n); \quad x_{n+1} = x_n + p_{n+1} \text{ mod } S; \quad (1)$$

where  $f(x) = -dV/dx = \epsilon \sin x$ . For sufficiently small  $\epsilon$ , there exist Kolmogorov-Arnold-Moser (KAM) invariant curves of (1) encircling the cylinder (i.e., ranging from  $x = 0$  to  $x = 2\pi$ ). These curves bound local-chaos regions which eventually merge into larger regions as  $\epsilon$  is increased, due to the breakup of the separating curves into cantori [3]. When the last curves break, for  $\epsilon = \epsilon_c \approx 0.9716$  [2], there emerges global chaos, i.e., a connected chaotic region encircling the cylinder and unbounded in the  $p$  direction. The average kinetic energy of an ensemble in this region grows diffusively,  $\langle p_n^2 \rangle = 2i / n$  [1,4]. For significantly larger than  $\epsilon_c$ , one observes superdiffusion of the global chaos,  $\langle p_n^2 \rangle = 2i / n^{1-\alpha}$  ( $1 < \alpha < 2$ ), due to accelerator-mode islands (AIs) [5,6]. Quantally, the kicked rotor exhibits dynamical localization in angular momentum [7], leading to a suppression of both the diffusion [7] and the superdiffusion [8]. The localization length in the superdiffusion case is strongly enhanced relative to the normal diffusion one [8]. All these phenomena have been observed in experimental realizations [9] of the quantum kicked rotor and related systems [10].

A basically different class of model systems are the kicked harmonic oscillators (KHOs) [11] with  $H = \frac{(u^2 + v^2)}{2} + \cos v \sum_{n=-1}^P \delta(t - n)$ , where  $\omega$  is the oscillator frequency and  $u$  and  $v$  are ordinary position and momentum variables. These systems describe periodically kicked charges in a uniform magnetic field [11-13] and are defined on the entire phase plane  $(u; v) \in \mathbb{R}^2$ . The values of  $w$  (column vector) at times  $t = n = 0$  are related by the "web" map  $w_{n+1}$  having the general canonical form

$$w : w_{n+1} = A [w_n + F(w_n)]; \quad (2)$$

where  $A = \begin{pmatrix} \cos \theta & \sin \theta \\ -\sin \theta & \cos \theta \end{pmatrix}$  is the matrix corresponding to a rotation by angle  $\theta$  and  $F(w)$  is a vector periodic function [for the Hamiltonian above,  $F(w) = (\sin v; 0)$ ]. In contrast with the usual kicked rotor, unbounded chaotic motion of  $w_n$  on a "stochastic web" is observed for arbitrarily small  $\theta$  [11-13]. In this weak-chaos regime, the diffusion on the web is essentially normal [12]. For  $q = 2, 3, 4, 6$ , the web has crystalline symmetry and Anderson localization arises for sufficiently large  $\theta$  [6]. A well-known example of (2) for  $q = 1$  ( $A = I$ ) is the map for the kicked Harper model (KHM) with  $H = \cos v + \cos u \sum_{n=1}^P (t_n)$  [13-15]. For  $\theta = \pi$ , the KHM exhibits a connected stochastic web like the  $q = 4$  KHO [16]. On the cylinder ( $u \in [0, 2\pi)$ ;  $v \in [0, 2\pi)$ ), such a web implies global chaos with normal diffusion for arbitrarily small  $\theta$ . For small  $\theta$  and with  $\theta$  sufficiently larger than  $1/n$ , one observes [14] a ballistic superdiffusion,  $\langle x^2 \rangle / n^2$ , due to "vertical" KAM curves in the  $p$  direction. Precisely because of these curves, however, this superdiffusion is not global: the angle variation is localized and does not encircle the cylinder. These and related classical features leave fingerprints in quantum-transport phenomena [14,15]. While the variety of these phenomena is quite rich and interesting, one should note that, unlike the kicked rotor, the KHM on the cylinder features an unrealistic expression  $\cos p$  for the kinetic energy.

In this Letter, we introduce a class of kicked rotors exhibiting Anderson localization and global superdiffusion for arbitrarily weak chaos. These systems correspond to standard maps (1) with

$$f(x) = K s(x) + g(x); \quad (3)$$

where  $K$  and  $\theta$  are parameters (the range of  $K$  is specified below),  $s(x)$  is the sawtooth function [ $s(x) = x$  for  $x \in [0, 2\pi)$  and  $s(x + 2\pi) = s(x)$ ], and  $g(x)$  is a general smooth  $2\pi$ -periodic function. For  $K > 0$  and  $\theta = 0$ ,  $f(x)$  corresponds to the hyperbolic sawtooth map which has been extensively studied as a completely chaotic system exhibiting unstable regular motion and resonances [3,17,18]. The case of integer  $K$  with  $\theta \neq 0$  corresponds to perturbed cat

maps (PCMs) which are smooth maps when defined on the  $2 \times 2$  torus [19]. Hyperbolic ( $K > 0$ ) PCMs have attracted much attention recently [19,20], especially in the context of "quantum chaos". Here we consider the standard map (1) with (3) in the perturbed elliptic case of  $-4 < K < 0$ . For  $\epsilon = 0$ , this map generically exhibits a pseudochaotic behavior (zero Lyapunov exponent) [21]; important exceptions, with regular elliptic motion, are the cases of integer  $K = 3; 2; 1$ . Examples of the perturbed case are shown in Fig. 1. In general, we show that this standard map is exactly related to a web map (2) taken modulo an "oblique" cylinder. For integer  $K$ , the orbit structure of  $T_\epsilon$  is essentially that of  $T_w$  folded back into the cylinder. Then, the existence of a stochastic web for  $T_w$  implies global chaos for  $T_\epsilon$ . The web skeleton on the cylinder is determined by a resonance Hamiltonian. For generic  $K$ , the global weak chaos arises as a perturbation of global pseudochaos. Now, it is known [17] that the unperturbed map  $T_\epsilon$  has stable accelerator-mode fixed points for  $K = 3$  and we show that this is generally the case for  $-4 < K < -2$ . For  $\epsilon = 0$  and small  $\epsilon$ , the AIs surrounding the fixed points are relatively large (see Fig. 1) and the global pseudochaos and weak chaos are strongly superdiffusive. For  $K = 3$ , the AIs are essentially normal web islands folded back into the cylinder and the superdiffusion emerges to a large extent by folding stochastic webs back into the cylinder. This weak-chaos superdiffusion thus appears to be basically different in nature from the strong-chaos one observed in the usual standard and web maps [5,6].

To establish an exact relation between  $T_\epsilon$  and  $T_w$ , consider first a map obtained from (1) by removing the mod  $S$  and by using (3) with  $s(x)$  replaced by  $x$ . This map, defined on the entire phase plane of  $z = (x; p)$ , can be written as follows:

$$z_{n+1} = B [z + G(z_n)]; \quad (4)$$

where the matrix  $B = \begin{pmatrix} K+1 & 1 \\ 1 & K \end{pmatrix}$  and  $G(z) = \begin{pmatrix} g(x) \\ 0 \end{pmatrix}$ . We denote by  $C = [z; \epsilon] \in [0; 1) \times [0; 1)$  the cylindrical phase space for  $T_\epsilon$  and define  $T_C$  as the map (4) with  $x_{n+1}$  (first equation) taken modulo  $S$ . Clearly, if we restrict ourselves to initial conditions

$z_0 \in C$ ,  $c = s$ . Now, for  $-4 < K < 0$ , it is easy to verify that  $B = Q^{-1}A Q$ , where  $A$  is the matrix for rotation by an angle determined by

$$2 \cos \theta = K + 2 \tag{5}$$

and  $Q = (k; k=2; 0; 1=2)$  with  $k = \tan(\theta/2)$ . Thus, the composition  $Q \circ Q^{-1}$  is precisely a web map (2) with  $w = (u; v) = Q^{-1} z$  and  $F(w) = Q^{-1} G(Q^{-1} w)$ . Explicitly,  $F(w) = (2)g(v+u=k)(k; 1)$ . The image of  $C$  under  $Q$  is an "oblique" cylinder  $C'$ , i.e., the strip bounded by the lines

$$v = \dots \quad u=k \tag{6}$$

with inclination angle  $\theta = (\dots) = 2$ . We define the web map "modulo  $C'$ " as

$$w_{n+1}^0 = w_n \text{ mod } C' : w_{n+1} = A^{-1} [w_n + F(w_n)] \text{ mod } w^0; \tag{7}$$

where  $w^0 = Q^{-1}(2; 0) = (2-k; 0)$  and  $m$  is the unique integer such that  $w_{n+1} \in C'$ . It is then easy to show that the following exact relation holds for all orbits with initial conditions  $z_0 \in C$  (or  $w_0 \in C'$ ):

$$s = c = Q^{-1} \frac{0}{w} Q. \tag{8}$$

It is well-known [19] that a map such as (4) can be defined consistently on the torus  $T^2 = [0; 1]^2$  only if  $B$  (and therefore  $K$ ) is integer. Only in this case two initial conditions  $z_0$  and  $z_0^0$  with  $(z_0 - z_0^0) \text{ mod } T^2 = 0$  will generate the same orbit under the torus map  $\tau_{T^2} = \text{mod } T^2$ . In addition,  $\tau_{T^2}$  is a smooth map (the discontinuity at  $x = 1$  is not felt, see Fig. 1 (a)) and the orbit structure of  $\tau_{T^2}$  is periodic in the phase plane with unit cell  $T^2$ . Obviously, it will be also periodic with "unit cell"  $C$  and the lift of  $\tau_{T^2}$  to  $C$  is precisely  $\tau_s$ . The cases of integer  $K = 3; 2; 1$  correspond, by Rel. (5), to  $q = 2 = 3; 4; 6$ , respectively. Due to  $w = Q^{-1} Q^{-1}$ , the periodicity of the orbit structure of  $\tau_{T^2}$  with unit cell  $T^2$  (or  $C$ ) in these cases implies a similar periodicity for  $\tau_w$  with unit cell  $T^2 = Q^{-1} T^2$  (or  $C'$ ). In fact, it can be easily seen that the map  $\tau_w^q, q = 3; 4; 6$ , is itself periodic with

unit cell  $T^2$  and its orbit structure has crystalline symmetry (triangular, square, hexagonal, respectively). One can then expect the generic existence of an extended chaotic orbit exhibiting this periodicity and symmetry. Such an orbit forms a "stochastic web", which has been observed for particular maps  $w$  [11,13]. In general, this web is a chaotic region encircling the torus  $T^2$  in two independent directions. This means that one has global chaos for the map (7) in  $C$  and, due to Rel. (8), also for  $s$  in  $C$ .

In the  $\epsilon \rightarrow 0$  limit, the orbits of  $w$  ( $q = 3; 4; 6$ ), in particular the stochastic web, form the energy contours of a "resonance" Hamiltonian  $H_0(w)$  [11], generating the flow to which the map  $w^q$  reduces as  $\epsilon \rightarrow 0$ . Since  $H_0(w)$ , like  $w^q$ , is periodic with unit cell  $T^2$ , one can consistently define the Hamiltonian determining the  $\epsilon \rightarrow 0$  orbit structure and web skeleton of  $s$  in  $T^2$  (or in  $C$ ) as  $H_0^0(z) = H_0(Qz)$ . In the case of  $K = 3$  ( $\nu = 2/3$ ) we obtain, using the notation  $h(x) = \int_{x_0}^x g(x^0) dx^0$ ,

$$H_0^0(z) = h(x) + h(x-p) + h(2x-p): \tag{9}$$

For example, in Fig. 1 (a) we observe a thin stochastic web encircling the torus  $T^2$  in the two directions and connecting the  $\nu$ -independent points of an unstable periodic orbit of period 3 with  $z_0 = (\pi/3; 0)$ . For this orbit, the value of (9), with  $h(x) = \cos x$ , is  $H_0^0 = 1$ . The web skeleton is then the energy contour  $H_0^0(z) = 1$ , indicated by the dotted line in Fig. 1 (a).

For noninteger values of  $K$ , the maps  $s$  and  $w$  exhibit no periodicity and there is no simple relation between the orbit structures of  $s$  and  $w$ . While a resonance Hamiltonian  $H_0(w)$  for  $w$  exists also for rational  $q \notin 3; 4; 6$  [11], it cannot be consistently defined for  $s$  in  $T^2$  or  $C$ . In the  $\epsilon = 0$  case, theoretical arguments and numerical evidence [21] strongly indicate that for irrational  $q$  the torus  $T^2$  can be partitioned into two regions having nonzero area: (a) A connected pseudochaotic region (zero Lyapunov exponent). (b) An apparently dense set of elliptic islands whose boundaries do not cross or touch the discontinuity line  $x = \pi/2$ . Because of the last fact, the pseudochaotic region encircles  $T^2$  in both the  $x$  and  $p$

directions, implying global pseudo-chaos in  $C$ . This will generally turn into global weak chaos when a small perturbation  $g(x)$  is applied. Fig. 1 (b) shows an example for  $\mu = (\sqrt{5} - 1)/2$  ( $K = 2.7247$ ) and  $\nu = 0.15$ .

Accelerator-mode fixed points (AFPs) of (1) satisfy  $p_1 - p_0 = 2^{-j}$  and  $x_1 = x_0 = p_1 - p_0 + 2^{-j^0}$ , where  $j$  and  $j^0$  are integers and  $j \neq 0$ . This implies that  $p_0$  is a multiple of  $2^{-j}$ . In the  $\nu = 0$  case, we find that  $x_0 = 2^{-j} - K$ . From the requirements that  $x_0$  must lie in the interval  $S = [0; 1)$  and corresponds to a stable AFP, it follows that  $jj = 1$  and  $x_0 = 2^{-j} - K$  with  $4 < K < 2$ . The latter condition on  $K$  is equivalent to  $2 < \mu < 3$ . For  $\nu = 0$  and for small  $\mu$ , the AIs surrounding the AFPs are relatively large (see Fig. 1). The observed pseudo-chaotic superdiffusion for  $\nu = 0$  is essentially ballistic ( $\langle n^2 \rangle = 2i / n$ ,  $\alpha = 2$ ) and the exponent in the weak-chaos regime is significantly larger than 1 (see Fig. 2). The AFPs and the AIs usually continue to exist also for large  $\mu$ . For example, the AFPs in Fig. 1 (a) undergo a period-doubling bifurcation at  $\mu = 1.3563$  and AIs and superdiffusion are observed at least up to  $\mu = 2$ , corresponding to a strongly chaotic regime. The size of the AIs and the exponent usually decrease as  $\mu$  is increased. For  $\mu = 2.2$ , an essentially normal diffusion ( $\alpha = 1$ ) is observed.

According to Eqs. (6)–(8), the AIs and the superdiffusion emerge when the web map  $w$  is taken modulo a cylinder  $C$  with  $2 < \mu < 3$  and inclination angle  $\theta = (\sqrt{5} - 1)/2$  ( $\theta = 4; 0$ ). This mechanism becomes most transparent in the integer case of  $K = 3$  ( $\mu = 6$ ), for which the orbit structure of  $w$  is periodic with unit cell  $T^2$  (or  $C$ ). In this case, the AIs are, up to the linear transformation  $Q$  in (8), just web islands folded back into  $C$  and the superdiffusion arises to a large extent by folding stochastic webs back into  $C$ . This is clearly illustrated in Fig. 3. We emphasize here that for small  $\mu$  the islands of  $w$  are all normal (nonaccelerating) and, in fact, we observe a perfectly normal diffusion on the phase plane of  $w$  (see, e.g., the dashed line in Fig. 2).

The weak-chaos superdiffusion thus appears to be basically different in nature from the strong-chaos one observed in both the usual standard map [ $f(x) = \sin x$ ] and the web map. The latter superdiffusion is totally due to the stickiness or trapping of chaotic orbits near the boundaries of AIs [5,6]. When the boundary island chain of an AI exhibits a self-similar islands-around-islands (IAIs) hierarchy, a renormalization-group approach predicts an exponent expressed entirely in terms of IAI scaling constants [6]. Suppose now that the AI boundary for the  $K = 3$  standard map  $s$  exhibits such an IAI hierarchy at some small value of  $\epsilon$ . Since the AIs are essentially normal islands of the related web map  $w$ , one may expect, naively, that a superdiffusion will take place under both maps  $s$  and  $w$  with the same exponent  $\nu > 1$ , contradicting the normal diffusion observed for  $w$ . This apparent paradox is resolved by noting that efficient trapping may not occur near the boundary of the web island and that the superdiffusion under  $s$  may not be totally due to IAI trapping. In fact, the results above indicate that it may be generally due to some combination of the "folding-back" mechanism with the IAI trapping, with the first mechanism dominating for very small  $\epsilon$ . We remark that inefficient trapping in self-similar IAI hierarchies has been observed in the usual standard map with the modulo in (1) taken with respect to  $p$  instead of  $x$  [22]. In this system, the superdiffusion in the angle  $x$  is mainly due to trapping in multilayered structures along rotational island chains and not to IAI trapping.

This work was partially supported by the Israel Science Foundation administered by the Israel Academy of Sciences and Humanities.

## REFERENCES

- [1] B.V. Chirikov, *Phys. Rep.* 52, 263 (1979)
- [2] J.M. Greene, *J. Math. Phys.* 20, 1183 (1979).
- [3] I.C. Percival, *AIP Conf. Proc.* 57, 302 (1979).
- [4] Y.H. Ichikawa, T. Kamimura, and T. Hatori, *Physica (Amsterdam)* 29D, 247 (1987).
- [5] R. Ishizaki, T. Horita, T. Kobayashi, and H. Mori, *Prog. Theor. Phys.* 85, 1013 (1991).
- [6] G.M. Zaslavsky, *Phys. Rep.* 371, 461 (2002), and references therein.
- [7] D.R. Gempel, R.E. Prange, and S. Fishman, *Phys. Rev. A* 29, 1639 (1984).
- [8] A. Iomin, S. Fishman, and G.M. Zaslavsky, *Phys. Rev. E* 65, 036215 (2002).
- [9] F.L. Moore, J.C. Robinson, C.F. Bharucha, B. Sundaram, and M.G. Raizen, *Phys. Rev. Lett.* 75, 4598 (1995); B.G. Klappauf, W.H. Oskay, D.A. Steck, and M.G. Raizen, *Phys. Rev. Lett.* 81, 4044 (1998); B. Fischer, A. Rosen, A. Bekker, and S. Fishman, *Phys. Rev. E* 61, R4694 (2000).
- [10] I. Dana, E. Eizenberg, and N. Shnerb, *Phys. Rev. E* 54, 5948 (1996).
- [11] G.M. Zaslavsky, R.Z. Sagdeev, D.A. Usikov, and A.A. Chernikov, *Weak Chaos and Quasi-Regular Patterns* (Cambridge University Press, 1991), and references therein.
- [12] A.J. Lichtenberg and B.P. Wood, *Phys. Rev. A* 39, 2153 (1989).
- [13] I. Dana and M. Amit, *Phys. Rev. E* 51, R2731 (1995).
- [14] R. Lima and D. Shepelyansky, *Phys. Rev. Lett.* 67, 1377 (1991); T. Geisel, R. Ketzmerick, and G. Petschel, *Phys. Rev. Lett.* 67, 3635 (1991); R. Artuso, G. Casati, F. Borgonovi, L. Rebuzzini, and I. Guameri, *Int. J. Mod. Phys. B* 8, 207 (1994), and references therein.
- [15] I.I. Satiya and B. Sundaram, *Phys. Rev. Lett.* 84, 4581 (2000); I.I. Satiya and T. Prosen,

- Phys. Rev. E 65, 047204 (2002).
- [16] In fact, the KHM is exactly related to generalized  $q = 4$  KHOs, see I. Dana, Phys. Lett. A 197, 413 (1995).
- [17] J.R. Cary and J.D. Meiss, Phys. Rev. A 24, 2664 (1981).
- [18] I. Dana, N.W. Murray, and I.C. Percival, Phys. Rev. Lett. 62, 233 (1989); Q. Chen, I. Dana, J.D. Meiss, N.W. Murray, and I.C. Percival, Physica (Amsterdam) 46D, 217 (1990); I. Dana, Phys. Rev. Lett. 64, 2339 (1990); 70, 2387 (1993).
- [19] J.P. Keating, F. Muzzadri, and J.M. Robbins, Nonlinearity 12, 579 (1999), and references therein; I. Dana, J. Phys. A 35, 3447 (2002).
- [20] M. Basilio de Matos and A.M. Ozorio de Almeida, Ann. Phys. 237, 46 (1995); M.V. Berry, J.P. Keating, and S.D. Prado, J. Phys. A 31, L245 (1998); J.P. Keating and F. Muzzadri, Nonlinearity 13, 747 (2000); I. Dana, Phys. Rev. Lett. 84, 5994 (2000); I. Dana and V.E. Chemov, Phys. Rev. E 67, 046203 (2003).
- [21] P. Ashwin, Phys. Lett. A 232, 409 (1997).
- [22] R.B. White, S. Benkadda, S. Katsirakis, and G.M. Zaslavsky, Chaos 8, 757 (1998).

## FIGURES

Fig. 1. Global chaos for the standard map (1) with (3),  $g(x) = \sin x$ , and: (a)  $K = 3$ ,  $\epsilon = 0.8$ ; (b)  $K = 2.7247498$ ,  $\epsilon = 0.15$ . The AIs are the regions indicated by elliptic orbits. The dotted line in (a) is the web skeleton from (9). The global chaos in (b) is a perturbation of global pseudochaos with an apparently dense set of islands.

Fig. 2. Dotted line:  $\ln(\overline{hE_n})$  versus  $\ln(n)$ ,  $E_n = e^{12} p_n^2 = 2$ , for the standard map defined in the caption of Fig. 1(a); the average  $\overline{h}$  is over an ensemble  $E$  of  $10^4$  initial conditions around  $(x = \pi/2; p = 0)$ ,  $n_{max} = 3 \cdot 10^4$ , and the linear fit (solid line) has slope  $\lambda = 1.56 \pm 0.03$ . Dashed line:  $\ln(\overline{hE_n})$  versus  $\ln(n)$ ,  $E_n = (u_n^2 + v_n^2) = 2$ , for the web map related to the standard map above by Rel. (8); the average  $\overline{h}$  is over the ensemble  $E^0 = Q \cup E$  ( $E$  is the ensemble above),  $n_{max} = 3 \cdot 10^4$ , and the slope of a linear fit is  $\lambda = 0.999 \pm 0.001$ .

Fig. 3. Stochastic web for the web map  $w$  related by (8) to the standard map defined in the caption of Fig. 1(a). The cylinder  $C$  is the oblique strip bounded by the parallel dashed lines. Together with these lines, the two horizontal dashed segments define the torus  $T^2$  in which there appear, essentially, the global chaos of Fig. 1(a). The first iteration of the "triangular" island  $0$  by  $w$  is island  $1$  which, when taken modulo  $C$ , is mapped into  $1^0$ . Continuing this process,  $1^0 \rightarrow 2^0 \rightarrow 3^0 \rightarrow 4^0 \rightarrow \dots$ . This shows how an AI  $0 \rightarrow 1^0 \rightarrow 2^0 \rightarrow \dots$  and the global superdiffusion emerge by folding web islands and stochastic webs back into  $C$  using (7).

This figure "fig1.jpg" is available in "jpg" format from:

<http://arxiv.org/ps/nlin/0304048v1>

Fig. 2

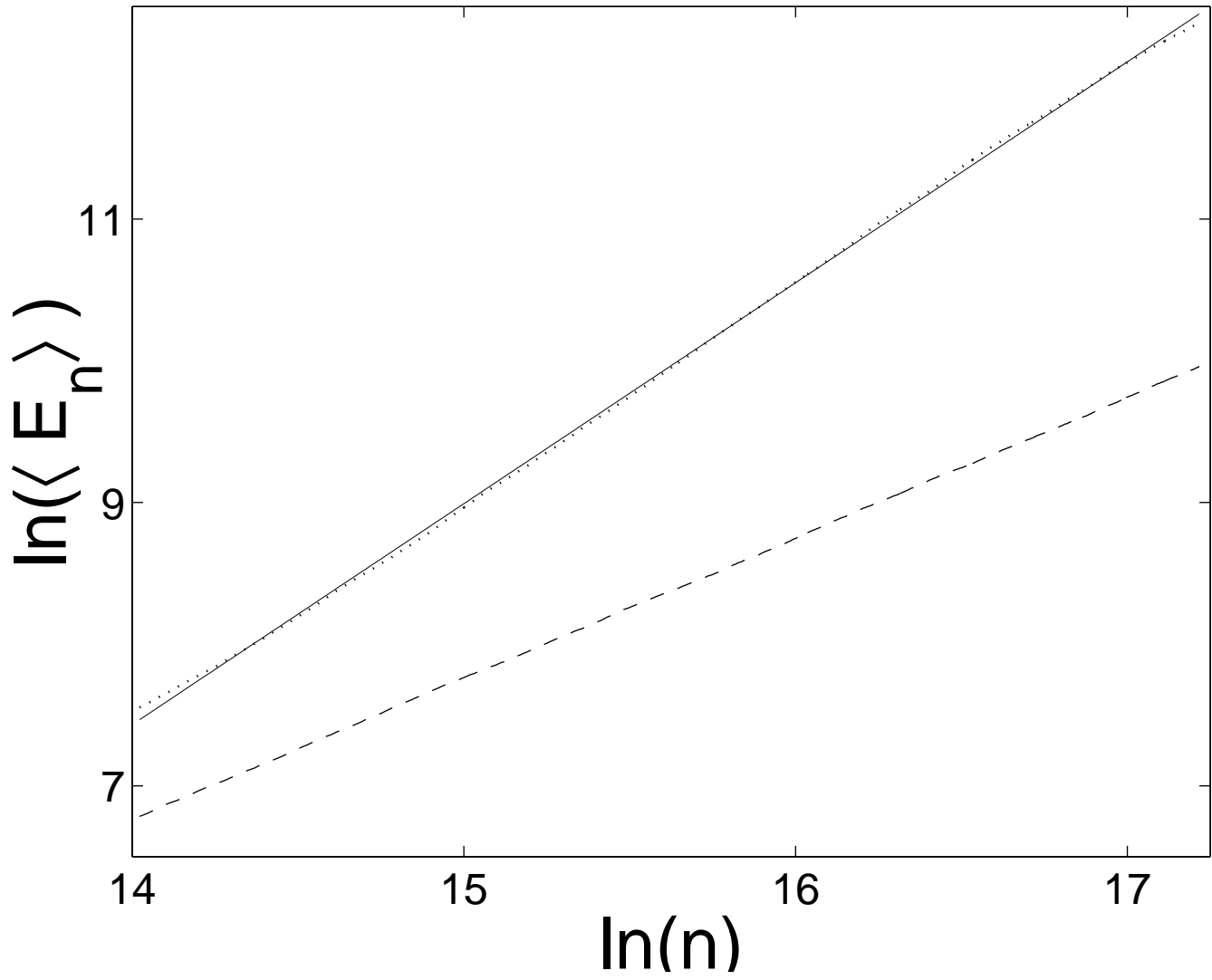


Fig. 3

